

李潇林斌,弓小平,马华东,等.西天山式可布台铁矿火山岩地球化学特征、成岩时代厘定及其构造意义[J].中国地质,2014,41(6): 1791–1804.
Li Xiaolinbin, Gong Xiaoping, Ma Huadong, et al. Geochemical characteristics and petrogenetic age of volcanic rocks in the Shikebutai iron deposit of West Tianshan Mountains[J]. Geology in China, 2014, 41(6): 1791–1804(in Chinese with English abstract).

西天山式可布台铁矿火山岩地球化学特征、成岩时代厘定及其构造意义

李潇林斌¹ 弓小平¹ 马华东² 韩 琼¹ 宋相龙¹ 谢 磊¹ 凤 骏¹ 王建设¹

(1.新疆大学地质与矿业工程学院,新疆 乌鲁木齐,830049;2.新疆国家三〇五项目办公室,新疆 乌鲁木齐,830000)

摘要:式可布台铁矿位于西天山阿吾拉勒铁矿成矿带西段,是此矿带极具代表性的铁矿床。主要赋存于以凝灰岩为主的石炭系上统伊什基里克组火山岩中。本文通过对式可布台矿区的火山岩进行岩石地球化学和LA-ICPMS锆石U-Pb测年分析来探讨火山岩形成的构造环境与成岩时代。地球化学分析表明大多数火山岩样品显示为高钾钙碱性系列;主量元素表明矿区火山岩主要由安山岩、英安岩、流纹英安岩组成,为钙碱性系列;微量元素和稀土元素表明矿区火山岩产出的构造环境为火山岛弧;LA-ICPMS锆石U-Pb测年显示火山岩的²⁰⁶Pb/²³⁸U加权平均年龄分别为(301±1)Ma和(313±2)Ma,表明该区的火山岩为晚石炭世早期。结合区域地质资料,认为矿区内出露的高钾钙碱性系列火山岩可能属于俯冲过程末期大陆岛弧岩浆作用的产物,其岩石的形成与构造岛弧环境有关,主体与下石炭统大哈拉军山组火山岩岩石学特征相似。

关 键 词:LA-ICPMS; 地球化学; 伊什基里克组; 式可布台铁矿; 西天山

中图分类号:P618.31;P588.14 **文献标志码:**A **文章编号:**1000-3657(2014)06-1791-14

西天山造山带是一个经历了复杂变形改造的晚古生代碰撞增生型造山带^[1],同时又是一个重要的成矿区域^[2-4],位于塔里木板块和准噶尔板块之间,被内部的伊犁地块分为南北两支(即:北天山缝合带和南天山缝合带),总体上呈弧形带状向东收敛展布^[5](图1-a)。自北向南可分为北天山弧增生地体、伊犁地块北缘活动陆缘、伊犁地块、伊犁地块南缘活动陆缘、中天山复合弧地体、西天山增生楔和塔里木北部被动大陆边缘^[6-8]。

阿吾拉勒山脉横亘于伊犁地块中部,区内石炭纪火山活动最为广泛(图1-c),自上而下依次为上

石炭统伊什基里克组火山岩、下石炭统阿克沙克组火山岩和大哈拉军山组火山岩,各组之间以角度不整合接触。伊什基里克组为一套以钙碱性系列为主,碱性系列次之的双峰式火山岩建造,其中玄武岩类以碱性为主^[9],该套地层为式可布台铁矿的赋矿地层;前人对大哈拉军山组火山岩研究较多,在其产出的构造环境方面存在较大争议,总结起来主要有“大陆裂谷-地幔柱说”^[10-11],“活动大陆边缘和岛弧说”^[12-16],“大陆减薄拉张说”^[17]3种观点。与之相比,对伊什基里克组火山岩的研究相对较少^[18-19],伊什基里克组的形成及演化与其下伏地层阿克沙

收稿日期:2014-11-05;改回日期:2014-11-17

基金项目:中国地质调查局项目“西天山阿吾拉勒成矿带铁矿成矿条件、成矿规律与勘查示范研究”子项目“西天山阿吾拉勒成矿带铁矿成矿条件与成矿规律研究”(资[2010]矿评01-03-26)和“西天山阿吾拉勒晚古生代火山作用与铁铜矿选区研究(12120123044000)”联合资助。

作者简介:李潇林斌,男,1989年生,硕士,主要从事地球探测与信息技术研究;E-mail:lb5310@sina.com。

通讯作者:弓小平,男,1963年生,博士,教授级高级工程师,从事综合信息成矿预测方面研究;E-mail:gxiaoping01@163.com。

克组、大哈拉军山组关系密切,其成因以及形成环境上缺乏可靠的地质依据。正确认识伊什基里克组火山岩的成因、形成环境,对研究西天山的地质演化和相关矿产勘查工作具有重要的理论和实践意义^[20]。对于伊什基里克组火山岩的成岩年代方面,该地层全岩 Rb-Sr 年龄为(317±16)Ma 和(318±8) Ma^[21],后来有学者运用锆石 SHRIMP 法获得其年龄为 313 Ma,其形成年龄较一致,但是对于式可布台铁矿在成岩成矿时代方面的未见相关报道。鉴于此,本文以式可布台铁矿为研究对象,对矿区内的矿体、围岩进行岩石地球化学方法和 LA-ICPMS 锆石 U-Pb 定年技术,探讨矿区火山岩的形成时代、构造环境以及式可布台铁矿的成岩成矿时代,为西天山构造演化的研究提供参考。

1 矿区地质概况

矿区地层由上石炭统伊什基里克组($C_2\gamma$)、新生界和第四系(Q_4)组成,其中上石炭统伊什基里克组为式可布台铁矿的赋矿围岩,其岩石类型主要有安山岩、层安山质火山角砾岩、层安山质凝灰岩、灰岩、安山凝灰质粉砂岩,为一套海相火山熔岩、火山碎屑岩夹泥质岩、碳酸盐岩的沉积建造。其顶、底均为火山喷发形成的碎屑岩-凝灰岩、凝灰质砂岩。碎屑岩中片理发育,近矿碎屑岩中片理密集、往两侧逐渐变弱,呈渐变过渡,最终过渡为正常沉积岩。含矿岩系的组合特征是:绢云母千枚岩-绢云母片岩-片理化凝灰岩-凝灰岩-凝灰质砂岩。岩性变化具有一定的韵律性,正常沉积岩中韵律性更明显。矿层多产出于岩性韵律变化的交替带或过渡带上,矿层与地层为整合接触。在铁矿层及顶底板常见有透镜状红碧玉、层纹状重晶石及石膏产出,产状与矿层一致。矿区发育 NWW 向和 NW 向脆性断裂,切割矿体。脆性断裂具有多期次的特征,主要由 NNW 向的断裂及其次生共轭断裂组成(图 1-b)。伊什基里克组火山岩的一段以复式背斜构造展布,与区域火山作用、岩浆作用、构造作用形式上表现出高度的一致性。

2 岩石地球化学特征

2.1 样品采集与分析方法

本次研究样品采自矿区出露较好具有代表性

的各种火山岩。样品新鲜,比较纯净,没有外来体的混入。每个样品重 2 kg 左右,共 8 件,进行主量、微量元素、稀土元素的测试分析。用于测试的样品经粗碎后再用碳化钨钵体磨成可过 200 目的粉末,每次换样品时均用自来水冲洗钵体并用酒精擦拭,防止样品间的混染。全岩主量元素采用 X 射线荧光法(XRF)在 X 荧光光谱仪上测定,测试将样品粉末熔成玻璃饼后用 X 射线荧光光谱(XRF)测试,测试精度优于 1%。烧失量(LOI)在烘烤箱中高温(1000℃)烘烤 90 min 获得。微量和稀土元素采用两酸(HNO₃+HF)高压反应釜溶样方法对样品粉末进行溶解。采用等离子质谱仪(ICP-MS; Agilent 7500a)来测定元素含量,含量高于 10×10⁻⁶ 元素的误差小于 5%,小于 10×10⁻⁶ 元素误差小于 10%。

用于 LA-ICPMS 锆石 U-Pb 的测试样品均采自新鲜火山岩。本次测试共 3 组样品,分别取自矿体底板凝灰岩(SK-Z004),坐标 E83°31'34.02", N43°31'40.07"; 矿体顶板凝灰质砂岩(SK-Z005)坐标 E83°38'33.34", N43°31'34.59"; 矿体顶板凝灰质砂岩(SK-Z006)坐标 E83°38'34.93", N43°31'35.03"。为保证测试需要,每个样品取样 3~5 kg。将样品送至河北省区域地质矿产调查研究所,样品经破碎后,用常规重力和磁选方法分选出锆石,在双目镜下挑纯; 将挑选出的锆石送至北京大学岩石矿床矿物研究所进行测年。将锆石样品和标样 TEM 置于环氧树脂上,磨平抛光,对锆石进行透射光和反射光显微照相以及阴极发光图像分析观察锆石结构,选择合适定位点进行测年和数据结果的分析和解释。锆石样品的 U-Th-Pb 同位素比值用标准锆石 91500 校正获得,单点分析的同位素比值及年龄误差为 1σ, 数据处理用 IsoPlot.3 软件完成^[23]。

2.2 主量元素

式可布台铁矿矿区火山岩样品硅酸盐测试结果(表 1)显示:SiO₂ 含量为 51.9%~66.5%, 火山岩全碱含量(Na₂O+K₂O)在 2.62%~7.27%, 平均含量为 4.79%。在火山岩 TAS 图解中(图 2-B), 样品主要落在安山岩、粗面安山岩、英安岩区域。Al₂O₃ 含量介于 9.82%~16.22%, 含量较高,且变化大; 在 SiO₂-Nb/Y 图解中(图 2-A), 大多数样品落入流纹英安岩/英安岩区内,个别样品落入安山岩和亚碱性安山岩区内,说明式可布台铁矿矿区火山岩为流纹英安

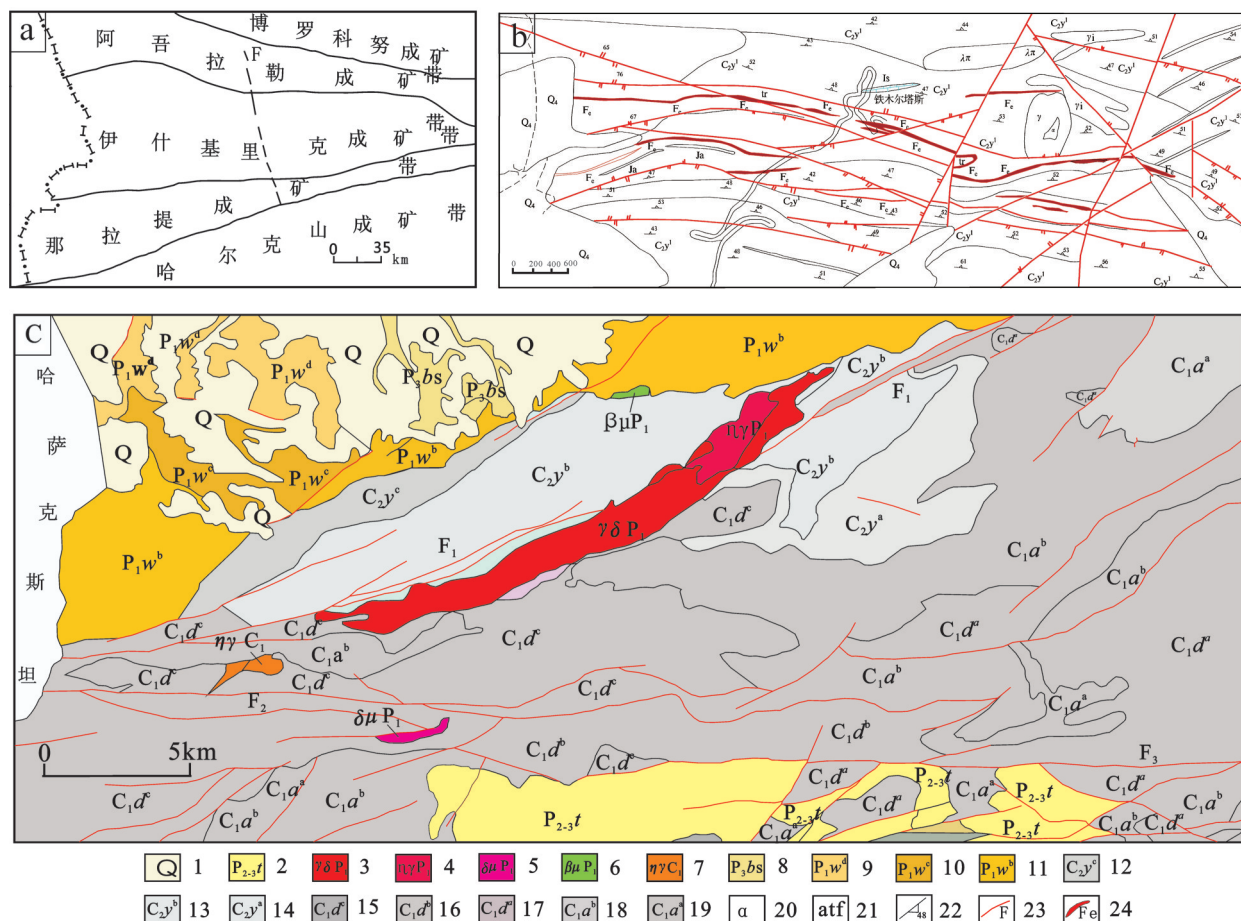


图1 研究区综合地质图(据文献[22]修改)

a—依什基里克成矿带略图;b—式可布台铁矿区域地质略图;c—依什基里克西段地质略图

1—第四系;2—新近系;3—早二叠世花岗闪长岩;4—早二叠世二长花岗闪长岩;5—早二叠世闪长玢岩;6—早二叠世辉绿玢岩;7—早石炭世二长花岗岩;8—下二叠统巴斯尔干组;9—下二叠统乌郎组第四段;10—下二叠统乌郎组第三段;11—下二叠统乌郎组第二段;12—中石炭统伊什基里克组第三段;13—中石炭统伊什基里克组第二段;14—中石炭统伊什基里克组第一段;15—下石炭统大哈拉军山组第三段;16—下石炭统大哈拉军山组第二段;17—下石炭统大哈拉军山组第一段;18—下石炭统阿克沙克组第二段;19—下石炭统阿克沙克组第一段;20—安山岩;21—安山质凝灰岩;22—片理产状;23—断层;24—铁矿层

Fig.1 Comprehensive geological map of the study area(modified after reference [22])

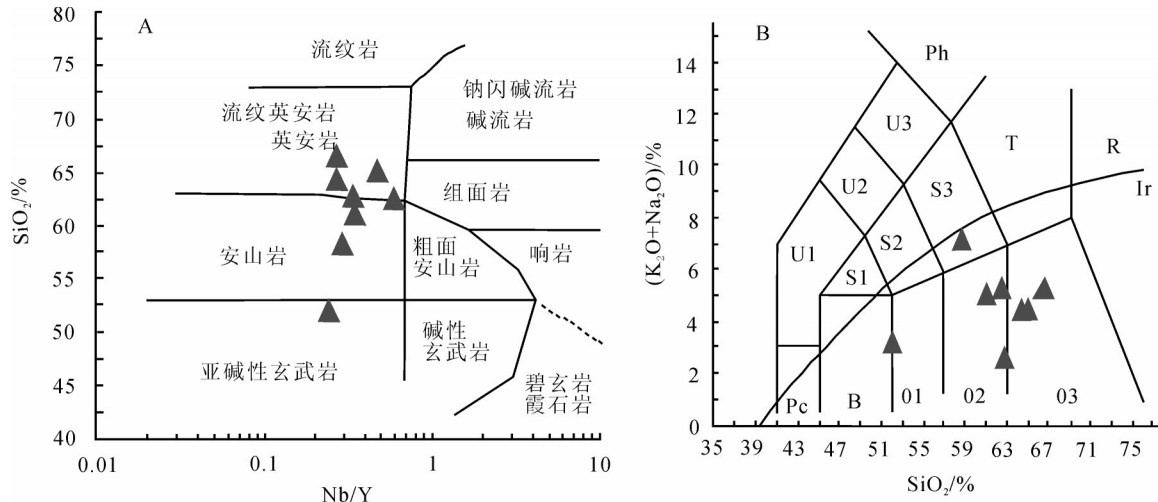
a—Sketch geological map of the Yishijilike metallogenic belt; b—Sketch geological map of the Shukebutai iron deposit;
c—Sketch geological map of western Yishijilike

1—Quaternary; 2—Neogene; 3—Early Permian granodiorite; 4—Early Permian monzonitic granodiorite; 5—Early Permian diorite porphyrite; 6—Early Permian allgavite; 7—Early Carboniferous monzonitic granite; 8—Lower Permian Basiergan Formation; 9—4th member of Lower Permian Wulang Formation; 10—3rd member of Lower Permian Wulang Formation; 11—2nd member of Lower Permian Wulang Formation; 12—3rd member of Middle Carboniferous Yishijilike Formation; 13—2nd member of Middle Carboniferous Yishijilike Formation; 14—1st member of Middle Carboniferous Yishijilike Formation; 15—3rd member of Lower Carboniferous Dahalajunshan Formation; 16—2nd member of Lower Carboniferous Dahalajunshan Formation; 17—1st member of Lower Carboniferous Dahalajunshan Formation; 18—2nd member of Lower Carboniferous Akshak Formation; 19—1st member of Lower Carboniferous Akshak Formation; 20—Andesite; 21—Andesitic tuff; 22—Attitude of schistosity; 23—Fault; 24—Iron ore bed

岩和英安岩系列。

测试结果中FeO含量为0~16.68%，其变化范围较大，引起变化的原因可能是由于采集的样品靠近矿体或者是受到后期的蚀变所引起的。MgO含量

为0.39%~3.15%，平均为1.66%。Fe₂O₃含量高变化大，变化范围为5.00%~20.22%，平均为10.92%，Na₂O含量低变幅度小，变化范围0.14%~4.5%，K₂O含量为2.44%~5.06%。TiO₂含量较低，变化范围为

图2 式可布台铁矿火山岩 SiO_2 -Nb/Y(A:底图据文献[24]修改)、TAS图解(B:底图据文献[25]修改)

Pc—苦橄玄武岩; B—玄武岩; 01—玄武安山岩; 02—安山岩; 03—英安岩; R—流纹岩; S1—粗面玄武岩; S2—玄武质粗面安山岩; S3—粗面安山岩; T—粗面岩、粗面英安岩; F—副长石岩; U1—碱玄岩; U2—响岩质碱玄岩; U3—碱质响岩; Ph—响岩; Ir—Irvine 分界线, 上方为碱性下方为亚碱性

Fig.2 SiO_2 -Nb/Y diagram of volcanic rocks in the Shikebutai iron deposit(Fig. A: modified after reference [24]), TAS diagram (Fig. B: modified after reference [25])

Pc—Picrite-basalt; B—Basalt; 01—Basaltic andesite; 02—Andesite; 03—Dacite; R—Rhyolite; S1—Trachybasalt; S2—Basaltic trachyandesite; S3—Trachyandesite; T—Trachyte, trachydacite; F—feldspathoidite; U1—Tephrite, basanite; U2—Phonolitic tephrite; U3—Pollenite; Ph—Phonolite; Ir—Irvine boundary , Upper part: alkaline; Lower part: subalkaline

0.32%~0.96%, 平均为0.61%。

2.3 稀土和微量元素

从式可布台火山岩样品的稀土、微量元素地球化学数据分析(表1)中可以看出:其稀土总量为 $\Sigma\text{REE}=48.26\times 10^{-6} \sim 426.04\times 10^{-6}$; $(\text{La}/\text{Yb})_N$ 为1.91~30.62,因此在稀土元素球粒陨石标准化分布形式图中(图3-A)样品呈现出较强的轻重稀土分馏,整体表现出轻稀土富集、重稀土亏损的右倾型配分模式; $(\text{La}/\text{Sm})_N$ 为2.16~7.40,所以轻稀土内部分馏相对较明显, $(\text{Gd}/\text{Yb})_N$ 为0.83~4.38,因此重稀土元素内部分馏较弱,配分曲线较为平坦;样品中铕表现出明显的正异常(δEu 为0.54~1.41)。 $(\text{Rb}/\text{Yb})_N$ 为24.63~100.87,平均50.06,这一比值明显区别于不相容元素强亏损($\text{Rb}/\text{Yb})_N < 1$ 的洋中脊玄武岩。岩石的Ta/Hf绝大部分大于0.1(0.08~0.29,平均0.16),显著有别于洋中脊玄武岩($\text{Ta}/\text{Hf} < 0.1$)。在微量元素原始地幔标准化蛛网图上(图3-B)多数岩石样品同样表现出类似的分配模式,表现为Th、Nd、Sm的强烈富集,K、Ti的亏损。

3 LA-ICPMS锆石U-Pb测年

本次测试样品中锆石为无色透明质浅黄色或

淡紫色呈正方双锥状、钮柱状及半截锥状,锆石晶体呈半自形到自形,粒径为0.05~0.2 mm不等,在CL阴极发光下锆石内部无明显包裹体和裂痕(图4),可见典型的岩浆韵律环带和明暗相间的条带结构等,个别出现扇形结构,可能是由于结晶过程中局部结晶生长速率发生变化所导致^[28]。属于岩浆结晶产物,锆石群形态单一,多数为喷发期岩浆活动一次结晶形成。

测试样品SK-Z004所挑选出的锆石中少部分可见黑色内核。从样品测试得到的同位素比值和年龄数据(表2)可见,锆石具有较高的Th/U比值,介于0.6093~1.6654,均大于0.1,反映锆石为典型岩浆成因^[29]。其中1、7样品年龄较其他样品年龄明显偏大,分别为1329 Ma和3334 Ma,出现这种现象的原因可能是测到了含有黑色内核锆石,代表的是岩浆的结晶年龄。加权平均结果为 $(313\pm 2)\text{Ma}$ (图5)。

在测试样品SK-Z005中挑选锆石进行测试,所得到的同位素比值和年龄数据可见,锆石具有较高的Th/U比值,分别介于0.4167~1.6654,均大于0.1,反映锆石为典型岩浆成因^[30]。其他样品的 $^{206}\text{Pb}/^{238}\text{U}$ 年龄介于298~321 Ma,加权平均结果为 $(301\pm 1)\text{Ma}$ (图6)。

表1 式可布台铁矿火山岩主量元素(%)、微量元素(10^{-6})、稀土元素(10^{-6})地球化学分析数据
Table1 Major elements(%), trace elements (10^{-6}) and rare earth elements (10^{-6}) compositions of volcanic rocks in the Shikebutai iron deposit

样品号	11SK-Z001	11SK-Z003	11SK-Z004	11SK-Z006	11SK-Z007	11SK-Z008	11SK-Z009	11SK-Z010
SiO ₂	51.90	62.80	62.50	66.50	61.05	65.06	64.29	58.22
TiO ₂	0.50	0.32	0.65	0.86	0.58	0.56	0.42	0.96
Al ₂ O ₃	9.83	9.82	15.65	15.74	15.89	16.22	12.01	16.2
Fe ₂ O ₃	20.22	20.00	10.79	7.92	6.18	5.00	5.42	11.79
TFe	16.68	0.05	1.70	0.00	2.73	2.00	0.93	3.45
MnO	1.05	0.27	0.08	0.40	0.15	0.11	0.07	0.07
MgO	1.40	0.39	1.51	0.60	3.15	2.76	1.19	2.24
CaO	0.63	0.22	0.56	0.28	3.17	2.13	5.86	1.39
Na ₂ O	0.14	0.18	0.85	0.18	2.65	1.94	2.14	4.50
K ₂ O	3.08	2.44	4.42	5.06	2.48	2.88	2.67	2.77
P ₂ O ₅	0.12	0.12	0.12	0.16	0.09	0.03	0.07	0.15
Ba	283	331	999	1960	447	498	171	508
Cr	31.1	29.9	38.5	164	71.20	20.60	1799	21.30
K	23400	18400	35300	41000	20200	23100	22100	21800
P	410	335	424	466	396	118	252	678
Th	1.20	5.90	9.70	6.70	8.30	9.60	5.36	5.00
Ti	3476	2126	4094	5080	3200	3059	2380	5471
Ta	0.56	0.43	1.56	0.57	0.62	0.60	1.09	0.26
Nb	7.60	8.00	9.90	10.75	8.3	9.1	8.30	6.80
Hf	5.06	3.50	5.64	7.09	4.18	4.34	3.80	2.36
Rb	86.20	79.10	232	226	111	127	80.60	77.40
Zr	128	102	162	224	156	159	119	74.90
Sr	9.00	18.8	19.6	26.38	268	272	50.38	112
Gd	4.80	5.50	1.90	5.50	3.90	3.90	11.40	6.40
Y	31.6	23.7	16.9	40.3	24.0	19.60	30.80	23.60
Sm	5.20	6.40	1.90	5.50	4.20	4.80	15.00	7.90
Nd	23.5	32.9	8.30	23.2	18.60	23.1	79.50	33.50
Sc	13.56	13.7	16.02	15.22	18.35	15.14	9.71	22.86
Ho	1.10	0.83	0.62	1.40	0.82	0.70	1.20	0.82
Ce	41.8	75.1	17.1	33.5	35.2	46.80	171	52.9
Er	3.20	2.30	1.90	3.90	2.3	1.90	2.80	2.10
Eu	1.40	2.80	0.51	2.00	0.98	1.20	2.40	2.70
Tm	0.52	0.35	0.34	0.64	0.38	0.31	0.38	0.29
Tb	0.82	0.88	0.37	1.00	0.66	0.61	1.50	0.95
Dy	5.00	4.40	2.50	6.00	3.90	3.30	6.80	4.60
Lu	0.64	0.39	0.42	0.74	0.45	0.33	0.46	0.33
La	22.4	45.5	8.10	11.9	17.80	23.80	111	26.60
Pr	5.40	8.40	2.00	4.90	4.40	5.60	20.00	7.10
Yb	3.50	2.20	2.30	4.20	2.50	1.90	2.60	1.80
ΣREE	119.28	187.95	48.26	104.38	96.09	118.25	426.04	147.99
LREE	99.7	171.1	37.91	81.00	81.18	105.30	398.90	130.70
HREE	19.58	16.85	10.35	23.38	14.91	12.95	27.14	17.29
LREE/HREE	5.09	10.15	3.66	3.46	5.44	8.13	14.70	7.56
(La/Yb) _N	4.32	13.98	2.38	1.91	5.11	8.99	30.62	10.60
(La/Sm) _N	4.30	7.10	4.30	2.16	4.24	4.96	7.40	3.37
(Gd/Yb) _N	1.37	2.50	0.83	1.31	1.56	2.05	4.38	3.56
(Rb/Yb) _N	24.63	35.95	100.87	53.81	44.40	66.84	31.00	43.00
δ Eu	0.84	1.41	0.81	1.10	0.73	0.82	0.54	1.12
δ Ce	0.87	0.85	0.97	1.03	0.95	0.96	0.82	0.92

注: $\delta Sr = [Ce_N / (Ce_N + Gd_N)]^{1/2}$; $\delta Eu = [Eu_N / (Eu_N + Gd_N)]^{1/2}$ 。

在测试样品 SK-Z006 所挑选的锆石中有少量锆石边部可见白色环带。从样品测试得到的同位

素比值和年龄数据可见, 锆石的 Th/U 比值同样较高, 分别介于 0.4701~2.6753, 均大于 0.1, 同样反映

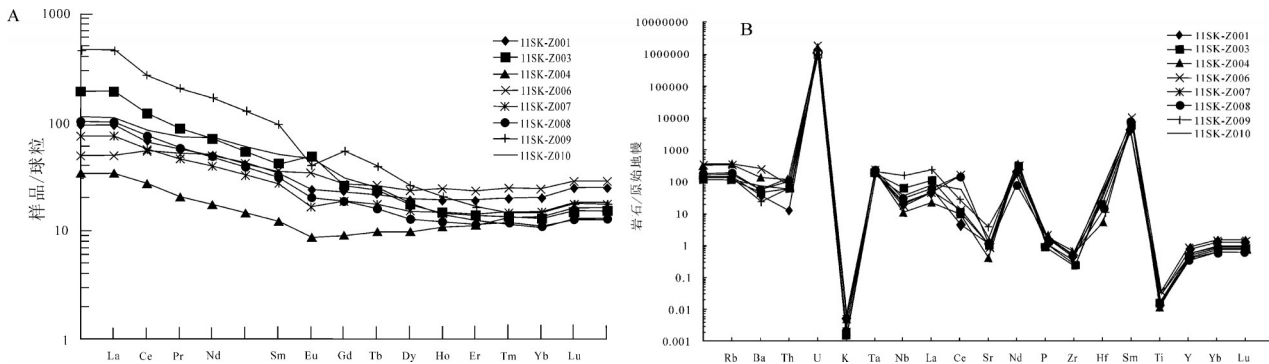


图3 稀土元素球粒陨石标准化分布形式图(图A:标准化值据文献[26]);微量元素原始地幔标准化蛛网图(图B:标准化值据文献[27])

Fig.3 Chondrite-normalized REE patterns (Fig. A: standardized value after reference [26]); Primitive mantle standardized spider diagram of trace elements (Fig. B: standardized value after reference [27])

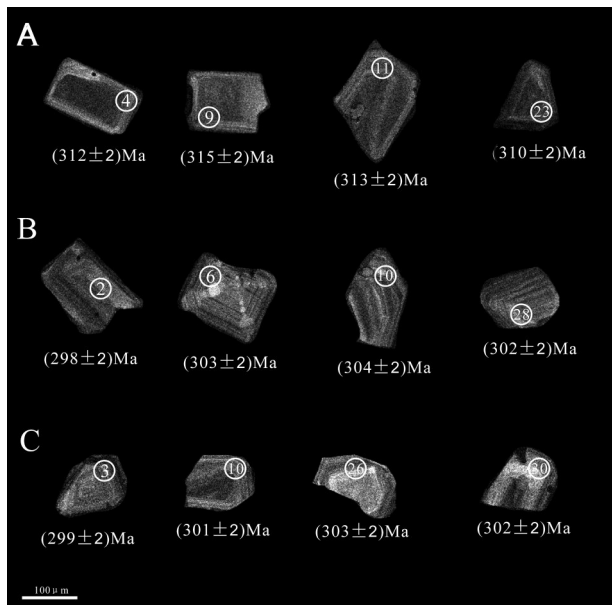


图4 式可布台铁矿测年锆石CL图像

A—样品SK-Z004:凝灰岩;B—样品SK-Z005:凝灰质砂岩;
C—样品SK-Z006:凝灰质砂岩

Fig.4 Cathodoluminescence images of zircons from the Shikebutai iron deposit

A—Sample SK-Z004: tuff; B—Sample SK-Z005: tuffaceous sandstone; C—Sample SK-Z006: tuffaceous sandstone

出锆石为典型岩浆成因。其中9、21、25号样品年龄明显比其他样品偏小,分别为192 Ma、199 Ma、165 Ma,出现这种现象的原因可能与一次Pb丢失的热事件有关。其他样品的²⁰⁶Pb/²³⁸U年龄介于258~320 Ma,加权平均值为(301±1)Ma(图7)。

4 讨 论

(1)在Nb/Y-SiO₂图解中(图2-A),大多数样品

落入流纹英安岩/英安岩区内说明式可布台铁矿矿区火山岩为流纹英安岩和英安岩系列;TAS图解(图2-B)和表1数据显示,该矿区的火山岩样品为高钾钙碱性系列,前人的研究认为这种高钾钙碱性—钾玄岩系列火山岩主要在俯冲过程的晚期阶段或者是构造体制由挤压转向碰撞后的伸展阶段出现^[31]。近年来,西天山东部其他地区也有晚石炭世高钾钙碱性火山岩的报道,暗示该地区的构造体制逐渐由挤压转变为伸展^[32]。

(2)计算得出FeO*/MgO变化范围为7.55~46.23,均大于2.0;K₂O/Na₂O变化范围为5.20~28.11,均大于0.6。哈克图解中TiO₂、Al₂O₃、Fe₂O₃、TFe、MnO、MgO、CaO、Na₂O、K₂O、P₂O₅含量与SiO₂之间整体上表现为较好的负相关性,表明岩浆可能经历了结晶分异演化作用;而K₂O和Na₂O的含量与SiO₂的相关性并不明显,则可能是由于在后期蚀变过程中的活动性所造成的。 $(\text{Na}_2\text{O}+\text{K}_2\text{O})/\text{Al}_2\text{O}_3$ 结果为0.27~0.45,由洪大卫标准 $(\text{Na}_2\text{O}+\text{K}_2\text{O})/\text{Al}_2\text{O}_3 < 0.9$ 为钙碱性岩石,说明式可布台铁矿为钙碱性岩石。TiO₂的平均为0.61%,明显与洋岛玄武岩(TiO₂平均含量大于2%)和洋脊玄武岩(TiO₂平均含量大于1.5%)不同,但与岛弧火山岩(TiO₂平均含量为0.8%)相接近。K₂O平均含量为3.22%,高于岛弧环境火山岩的含量(K₂O的平均1.60%),而与活动陆缘K₂O含量接近^[33~35]。总体看来式可布台铁矿具有活动陆缘岛弧的特点。

(3)稀土微量元素分析表明式可布台火山岩稀土元素配分形式整体表现为向右倾斜的轻稀土明显富集,重稀土弱亏损。LREE/HREE为3.46~

表2 式可布台铁矿火山岩样品 LA-ICPMS 锆石 U-Pb 定年分析结果
 Table 2 LA-ICPMS zircon U-Pb isotopic data of volcanic rock samples from the Shikebutai iron deposit

样品号	含量/ 10^6	同位素比值										年龄/Ma										
		Pb	U	$^{206}\text{Pb}/^{238}\text{U}$	1σ	$^{207}\text{Pb}/^{235}\text{U}$	1σ	$^{207}\text{Pb}/^{206}\text{Pb}$	1σ	$^{208}\text{Pb}/^{232}\text{Th}$	1σ	$^{232}\text{Th}/^{238}\text{U}$	1σ	$^{206}\text{Pb}/^{238}\text{U}$	1σ	$^{207}\text{Pb}/^{235}\text{U}$	1σ	$^{207}\text{Pb}/^{206}\text{Pb}$	1σ	$^{207}\text{Pb}/^{238}\text{U}$	1σ	
SK-Z004-1	43.0	194	0.2289	0.0015	2.7464	0.0300	0.0870	0.0005	0.0141	0.0003	0.6881	0.0044	1329	9.00	1341	15.0	1361	11.0				
SK-Z004-4	3.00	55.0	0.0495	0.0003	0.3618	0.0083	0.0530	0.0025	0.0126	0.0001	0.7941	0.0070	312	2.00	314	7.00	328	106				
SK-Z004-7	6.20	81.0	0.6774	0.0041	26.5832	0.6571	0.2846	0.0016	0.0126	0.0003	0.9459	0.0068	3334	20.00	3368	83.0	3389	9.0				
SK-Z004-9	14.0	240	0.0500	0.0003	0.3539	0.0031	0.0528	0.0007	0.0114	0.0002	1.1946	0.0062	315	2.00	315	3.00	319	30.0				
SK-Z004-10	14.0	255	0.0498	0.0003	0.3615	0.0071	0.0526	0.0008	0.0139	0.0003	0.7825	0.0049	313	2.00	313	6.00	313	35.0				
SK-Z004-11	5.00	91.0	0.0498	0.0003	0.3656	0.0137	0.0533	0.0026	0.0154	0.0003	0.6588	0.0059	313	2.00	316	12.0	340	109				
SK-Z004-18	16.0	269	0.0497	0.0003	0.3860	0.0095	0.0563	0.0007	0.0127	0.0003	1.2298	0.0064	313	2.00	331	8.00	465	26.0				
SK-Z004-23	4.00	76.0	0.0493	0.0004	0.3248	0.0074	0.0537	0.0024	0.0130	0.0003	0.8801	0.0045	310	2.00	316	6.00	357	102				
SK-Z004-28	6.00	105	0.0496	0.0004	0.3277	0.0109	0.0545	0.0017	0.0144	0.0003	0.6093	0.0040	312	2.00	322	9.00	393	69.0				
SK-Z005-2	13.0	247	0.0474	0.0003	0.3477	0.0039	0.0533	0.0005	0.0165	0.0001	0.7346	0.0118	298	2.00	303	3.00	340	23.0				
SK-Z005-3	5.00	91.0	0.0483	0.0003	0.3527	0.0055	0.0530	0.0008	0.0145	0.0001	0.9402	0.0060	304	2.00	307	5.00	328	34.0				
SK-Z005-6	9.00	169	0.0481	0.0003	0.3506	0.0068	0.0528	0.0010	0.0166	0.0001	0.5409	0.0047	303	2.00	305	6.00	322	44.0				
SK-Z005-7	21.0	412	0.0475	0.0003	0.3524	0.0104	0.0539	0.0013	0.0132	0.0003	0.7611	0.0038	299	2.00	307	9.00	365	56.0				
SK-Z005-8	4.00	78.0	0.0473	0.0003	0.3568	0.0066	0.0548	0.0009	0.0175	0.0002	0.8884	0.0045	298	2.00	310	6.00	403	37.0				
SK-Z005-9	4.00	71.0	0.0482	0.0003	0.3512	0.0033	0.0529	0.0005	0.0172	0.0002	0.6846	0.0035	303	2.00	306	3.00	324	22.0				
SK-Z005-10	8.00	150	0.0483	0.0003	0.3556	0.0102	0.0534	0.0014	0.0180	0.0003	0.5088	0.0032	304	2.00	309	9.00	346	59.0				
SK-Z005-14	3.00	57.0	0.0476	0.0003	0.3476	0.0067	0.0529	0.0010	0.0174	0.0004	0.7341	0.0064	300	2.00	303	6.00	327	42.0				
SK-Z005-15	7.00	102	0.0477	0.0003	0.3467	0.0106	0.0527	0.0015	0.0182	0.0001	1.3116	0.0186	301	2.00	302	9.00	315	66.0				
SK-Z005-16	4.00	63.0	0.0480	0.0008	0.3476	0.0093	0.0525	0.0014	0.0182	0.0003	0.7791	0.0039	302	2.00	303	8.00	309	59.0				
SK-Z005-17	4.00	80.0	0.0473	0.0003	0.3473	0.0067	0.0533	0.0010	0.0199	0.0003	0.5843	0.0032	298	2.00	303	6.00	340	41.0				
SK-Z005-26	6.00	105	0.0484	0.0003	0.3526	0.0020	0.0529	0.0003	0.0201	0.0004	0.5019	0.0035	305	2.00	307	2.00	323	15.0				
SK-Z005-28	5.00	90.0	0.0480	0.0004	0.3532	0.0113	0.0534	0.0016	0.0199	0.0003	0.6315	0.0037	302	2.00	307	10.0	344	68.0				

续表2

样品号	Pb	U	$^{206}\text{Pb}/^{238}\text{U}$	同位素比值				年龄/Ma										
				$^{207}\text{Pb}/^{235}\text{U}$	1σ	$^{207}\text{Pb}/^{206}\text{Pb}$	1σ	$^{232}\text{Th}/^{232}\text{Th}$	1σ	$^{206}\text{Pb}/^{238}\text{U}$	1σ	$^{207}\text{Pb}/^{235}\text{U}$	1σ					
SK-Z00529	4.00	72.0	0.0478	0.0004	0.3578	0.0064	0.0543	0.0009	0.0223	0.0003	0.4936	0.0025	301	2.00	311	6.00	385	37.0
SK-Z0062	4.00	78.0	0.0475	0.0003	0.3456	0.0130	0.0527	0.0020	0.0197	0.0001	0.7395	0.0037	299	2.00	301	11.0	318	85.0
SK-Z0063	11.0	196	0.0475	0.0003	0.3717	0.0063	0.0567	0.0010	0.0177	0.0001	0.6713	0.0053	299	2.00	321	5.00	480	38.0
SK-Z0064	23.0	408	0.0477	0.0003	0.3525	0.0029	0.0536	0.0005	0.0175	0.0001	0.9131	0.0053	300	2.00	307	3.00	356	20.0
SK-Z0065	6.00	115	0.0475	0.0003	0.3475	0.0129	0.0531	0.0020	0.0170	0.0002	0.8672	0.0045	299	2.00	303	11.0	332	83.0
SK-Z0066	18.0	300	0.0481	0.0003	0.3492	0.0046	0.0526	0.0007	0.0170	0.0001	0.9781	0.0062	303	2.00	304	4.00	312	30.0
SK-Z0067	6.00	107	0.0475	0.0003	0.3461	0.0124	0.0529	0.0018	0.0177	0.0003	1.0028	0.0062	299	2.00	302	11.0	324	78.0
SK-Z0069	10.00	265.0	0.0302	0.0002	0.2131	0.0033	0.0512	0.0008	0.0052	0.0002	2.6753	0.0223	192	2.00	196	3.00	251	36.0
SK-Z00610	10.0	184	0.0478	0.0003	0.3461	0.0075	0.0525	0.0011	0.0172	0.0003	0.8145	0.0053	301	2.00	302	7.00	307	49.0
SK-Z00612	15.0	271	0.0479	0.0003	0.3467	0.0042	0.0525	0.0007	0.0167	0.0001	0.8578	0.0066	301	2.00	302	4.00	309	30.0
SK-Z00613	16.0	296	0.0476	0.0003	0.3475	0.0050	0.0529	0.0008	0.0161	0.0001	0.7687	0.0039	300	2.00	303	4.00	326	34.0
SK-Z00614	3.00	57.0	0.0477	0.0003	0.3473	0.0199	0.0528	0.0030	0.0189	0.0004	0.6538	0.0033	300	2.00	303	17.0	320	128
SK-Z00615	5.00	86.0	0.0477	0.0003	0.3491	0.0155	0.0531	0.0023	0.0176	0.0001	0.8198	0.0055	300	2.00	304	14.0	332	98.0
SK-Z00617	5.00	85.0	0.0480	0.0003	0.3492	0.0246	0.0528	0.0036	0.0195	0.0003	0.5898	0.0029	302	2.00	304	21.0	320	155
SK-Z00619	6.00	110	0.0476	0.0003	0.3502	0.0174	0.0533	0.0026	0.0205	0.0004	0.5993	0.0042	300	2.00	305	15.0	342	112
SK-Z00620	5.00	84.0	0.0480	0.0004	0.3489	0.0243	0.0527	0.0036	0.0200	0.0003	0.6872	0.0034	302	2.00	304	21.0	315	156
SK-Z00621	27.0	686	0.0313	0.0002	0.2229	0.0015	0.0517	0.0004	0.0115	0.0003	1.1185	0.0058	199	1.00	204	1.00	271	19.0
SK-Z00622	4.00	74.0	0.0480	0.0003	0.3482	0.0148	0.0526	0.0023	0.0196	0.0003	0.6364	0.0048	302	2.00	303	13.0	311	98.0
SK-Z00624	10.0	169	0.0480	0.0003	0.3527	0.0064	0.0533	0.0010	0.0177	0.0003	0.8436	0.0066	302	2.00	307	6.00	341	42.0
SK-Z00625	41.0	808	0.0259	0.0002	0.1788	0.0009	0.0501	0.0003	0.0151	0.0003	2.0562	0.0104	165	1.00	167	1.00	200	15.0
SK-Z00626	11.0	159	0.0481	0.0003	0.3490	0.0083	0.0526	0.0013	0.0206	0.0004	1.2595	0.0082	303	2.00	304	7.00	310	55.0
SK-Z00630	4.00	81.0	0.0480	0.0003	0.3565	0.0179	0.0539	0.0027	0.0226	0.0003	0.5089	0.0025	302	2.00	310	16.0	366	113

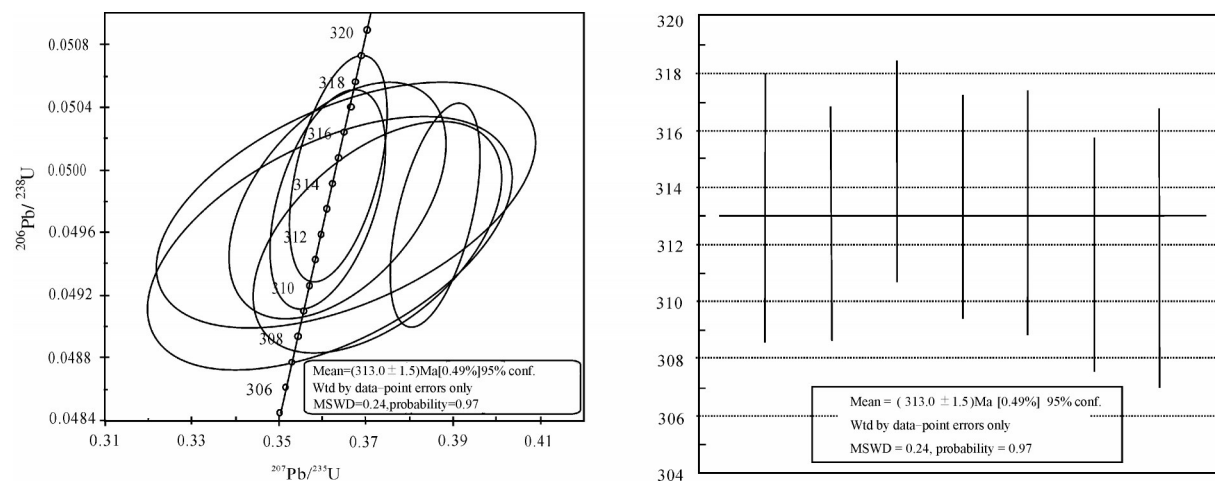


图5 式可布台铁矿SK-Z004号样品锆石U-Pb年龄谐和图、直方图

Fig.5 U-Pb age concordia diagram and histogram of zircon sample SK-Z004 from the Shikebutai iron deposit

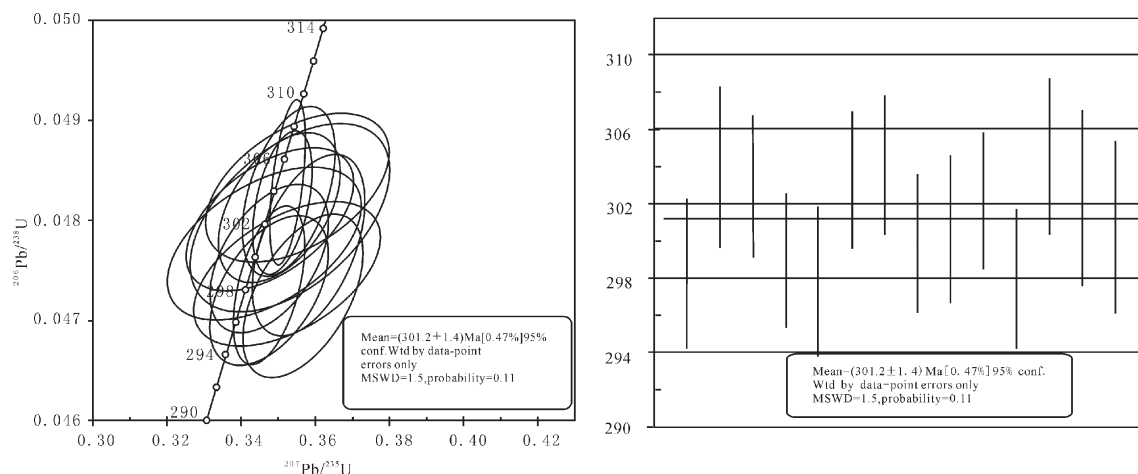


图6 式可布台铁矿SK-Z005号样品锆石U-Pb年龄谐和图、直方图

Fig.6 U-Pb age concordia diagram and histogram of zircon sample SK-Z005 from the Shikebutai iron deposit

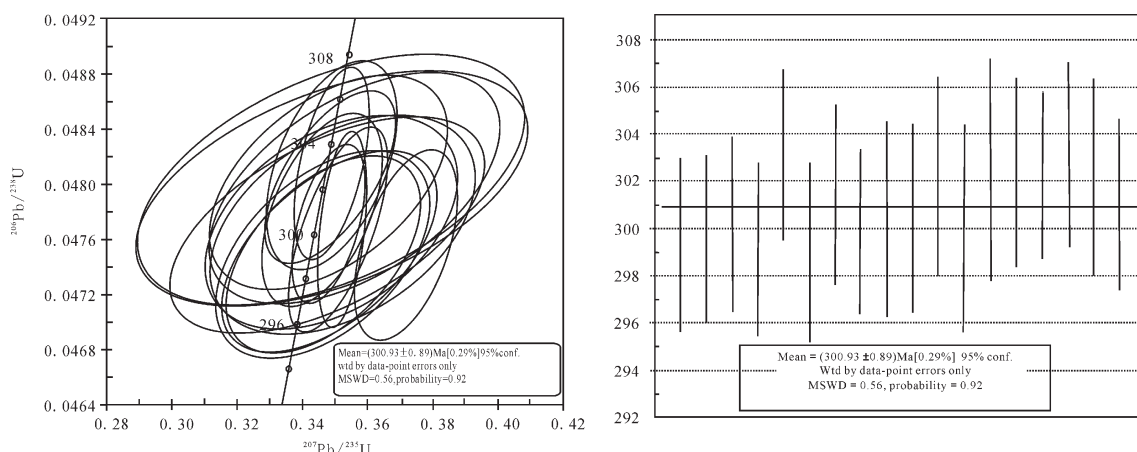


图7 式可布台铁矿SK-Z006号样品锆石U-Pb年龄谐和图、直方图

Fig.7 U-Pb age concordia diagram and histogram of zircon sample SK-Z006 from the Shikebutai iron deposit

14.70, 平均为7.27, 其比值较小, 表示岩浆分异程度较强。稀土配分曲线曲线吻合程度较好, 反映属同一岩浆房的产物。 Σ REE及LREE/HREE变化范围大, 显示火山岩浆的演化长期性和多期次性, 或是双峰式特征的体现。除3个样品外, 余5样品的 δ Eu均<1, 其值为0.54~0.84, 平均0.62, 为铕弱负异常(铕弱亏损型), 表明岩浆分异程度较高。 $(La/Sm)_N$ 比值均大于1, 比值为2.16~7.4, 平均为4.73, 反映轻稀土之间分馏程度较好。 $(Gd/Yb)_N$ 为0.83~4.38, 平均为2.20, 其值较大, 说明重稀土之间分馏不明显。 δ Ce比值除一个样品大于1, 其余样品小于1, 平均为0.92, 显示地壳岩石特征。 $(La/Yb)_N$ 比值为1.91~30.62, 平均值为9.74, 因而稀土配分曲线为右陡倾式。Sr亏损的原因可能是斜长石发生分离结晶也可能是因为交代蚀变作用使Sr发生迁移的结果^[36~37], 但由于本次样品主要属于中基性火山岩不太可能发生斜长石的分离结晶, 加之Eu表现出明显的正异常, 故Sr的亏损可能是由于交代蚀变作用使Sr发生迁移的结果。此外, 本次研究测试的数据中大多数样品显示Ba元素的富集, 只有个别样品显示Ba元素的亏损, 该特征与南阿尔卑斯二叠纪的高钾钙碱性火山岩类似, 通过对比, 说明西天山阿吾拉勒一带经历了由俯冲碰撞造山的挤压转向后碰撞

的伸展拉张的构造体制变更, 本次研究矿区火山岩的形成时代为300~313 Ma, 结合西天山的构造演化历史, 说明式可布台铁矿矿区火山岩形成的构造环境为火山岛弧。

(4)在Th-Hf-Ta图(图8-B)中可以看出, 样品大部分落在代表火山弧玄武岩的CAB区, 其构造环境可能属于岛弧环境, 根据Hf/Th的比值为0.045~1.06, 均小于3, 可以进一步将落在CAB区的样品划分为钙-碱性玄武岩^[38~39]。在Th-Hf-Ta图解中(图8-B), 大多数样品落在IAT区内, 在MnO-TiO₂-P₂O₅(图8-A)样品大多数落在CAB区内, 并且向IAT演化的趋势, 综合两个图解, 可以说明式可布台铁矿火山岩的形成与构造岛弧环境有关。

(5)北天山古洋盆的关闭时间, 一直存在较大的争议。北天山蛇绿混杂岩带沿北天山北缘断裂两侧呈NWW-SEE向展布, 向东可断续延入东天山干沟一带。侵入其中的四棵树花岗岩体具钉合岩体意义^[40], 岩体中部花岗闪长岩的SHRIMP锆石U-Pb年龄为(316±3)Ma, 很好地限定了北天山洋的闭合时间^[41]。近年来的区调成果认为北天山其南部的依连哈比尔尕岩基为晚石炭世(280~310 Ma)同碰撞花岗岩, 确定该洋盆闭合时代应在310 Ma之前^[42]。笔者此次LA-ICPMS锆石U-Pb测年结果分

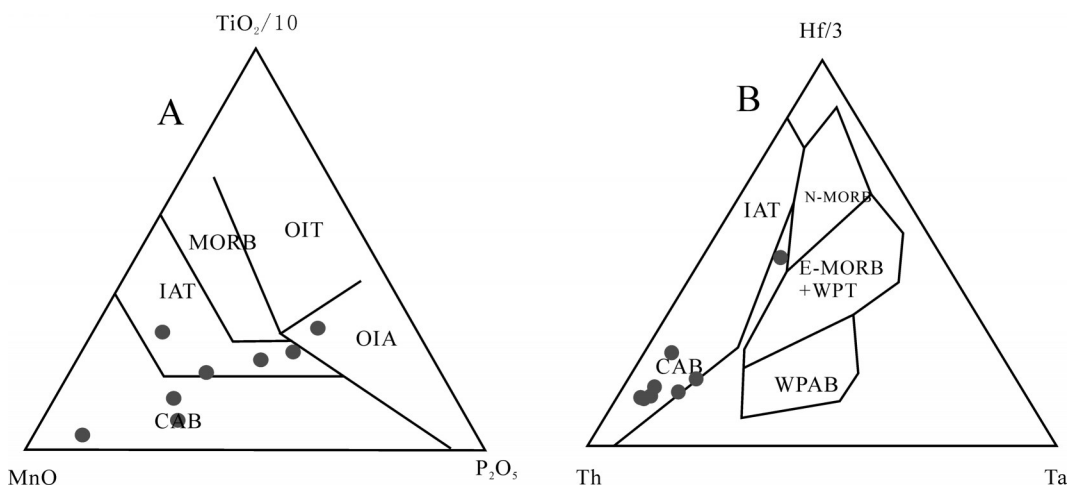


图8 式可布台铁矿火山岩MnO-TiO₂-P₂O₅图解(图A:标准化值据文献[49])和Th-Ta-Hf三角图(B:标准化值据文献[50])

OIT—洋岛拉斑玄武岩; OIA—洋岛碱性玄武岩; MORB—洋中脊玄武岩; IAT—岛弧拉斑玄武岩; CAB—钙碱性玄武岩
Fig.8 MnO-TiO₂-P₂O₅ diagram (Fig. A: standardized value after reference [49]) and Th-Ta-Hf triangular diagram (Fig. B: standardized value after reference [50]) of the Shikebutai iron deposit

OIT—Oceanic island tholeiite; OIA—Ocean island alkali-basalts; MORB—Mid-ocean ridge basalts; IAT—Island arc tholeiite; CAB—Calc-alkali basalt

别显示为 (313 ± 2) Ma、 (301 ± 1) Ma、 (301 ± 1) Ma, 均属于晚石炭世, 该数据与316 Ma接近^[45], 这也从侧面为北天山洋的闭合时间在晚石炭世提供了时间上的依据。区域地质资料表明在石炭纪末—早二叠世($260\sim300$ Ma), 西天山地区的构造体制开始由俯冲碰撞造山的挤压转向后碰撞的伸展拉张^[43~44], 具体表现为天山南北缘及伊犁盆地出现多个火山盆地, 喷发大量的陆相双峰式火山岩同时伴有富钾花岗岩的侵入^[45]。

样品SK-Z004测试结果中, 1、7点年龄较其他样品年龄明显偏大, 分别为1329 Ma和3334 Ma, 出现这种现象的原因可能是所测试样品中含有黑色内核锆石, 该锆石代表的是岩浆的结晶年龄。这与李继磊等所研究的北天山存在前寒武纪基底的结论相一致: 北天山区域前寒武系包括古元古界温泉群、中元古界哈尔达坂群和特克斯群、新元古界开尔塔斯群、库松木切克群和科克苏群, 主要分布在北天山北部和南部, 哈萨克斯坦东南部Anrankhal山Uzunbulak花岗片麻岩的锆石U-Pb年龄为2791 Ma, Erektas河花岗片麻岩的锆石U-Pb年龄为1789 Ma^[46], 阿吾拉勒西段片麻岩锆石U-Pb年龄为1609 Ma^[47]。从侧面证明了伊犁地块前寒武纪基地是存在的^[48]。

结合区域地质资料分析, 在晚石炭世, 西天山北天山洋盆闭合, 伊犁地块南北缘成为增生造山带, 地壳加厚, 形成大量富铝花岗岩, 伊犁盆地内部由挤压环境逐渐向拉张环境过渡, 一定的构造组合型式反映了一定地质条件下某种特定的地壳变形方式, 所以它们在控岩控矿方面也有类似的作用。从而在阿吾拉勒山和乌孙山形成大量钙碱性和碱性火山岩共存的海陆交互伊什基里克组, 继承了大哈拉军山组钙碱性特征, 相关资料显示, 其下部有未出露的超基性岩, 可能已拉张到一定程度^[51]。在西天山构造演化过程中, 为式可布台铁矿成矿物质的富集和运移等提供了良好的构造条件, 同时伊什基里克组特定的岩石组合及其形成环境也为成矿提供了物源基础。

5 结 论

(1) 式可布台赋矿围岩伊什基里克组火山岩岩石地球化学特征为活动陆缘岛弧的特点, 主体与下

石炭统大哈拉军山组火山岩岩石化学特征相似。

(2) LA-ICPMS锆石U-Pb定年结果显示式可布台铁矿火山岩同位素年龄为301~313 Ma, 表明式可布台铁矿火山岩形成时代为晚石炭世早期。

(3) 矿区内301~313 Ma的高钾钙碱性系列火山岩可能属于俯冲过程末期阶段大陆岛弧岩浆作用的产物, 其具体的岩浆源区与演化过程仍需要进一步的同位素方面的研究。

参 考 文 献(References):

- [1] Windley B, Allen M, Zhang C, et al. Paleozoic accretion and Cenozoic reformation of the Chinese Tien Shan Range[J], Central Asia.Geology, 1990, 18(2): 128~131.
- [2] 朱永峰, 何国琦, 安芳. 中亚成矿域核心地区地质演化与成矿规律[J]. 地质通报, 2007, (09): 1167~1177.
Zhu Yongfeng, He Guoqi, An fang. Geological evolution and metallogeny in the core part of the Central Asian metallogenic domain[J]. Geological Bulletin of China, 2007, (09): 1167~1177 (in Chinese with English abstract).
- [3] 朱永峰, 周晶, 郭璇. 西天山石炭纪火山岩岩石学及Sr-Nd同位素地球化学研究[J]. 岩石学报, 2006, 05: 1341~1350.
Zhu Yongfeng, Zhou Jing, Guo Xuan.Petrology and Sr- Nd isotopic geochemistry of the Carboniferous volcanic rocks in the western Tianshan Mountains, NW China[J]. Acta Petrologica Sinica, 2006, 05: 1341~1350 (in Chinese with English abstract).
- [4] 朱永峰, 周晶, 宋彪, 等. 新疆“大哈拉军山组”火山岩的形成时代问题及其解体方案[J]. 中国地质, 2006, 03: 487~497.
Zhu Yongfeng, Zhou Jing, Song Biao, et al. Age of the “Dahalajunshan” Formation in Xinjiang and its disintegration[J]. Geology in China, 2006, 03: 487~497(in Chinese with English abstract).
- [5] 王作勋, 邬继易, 吕喜朝, 等. 中国天山板块构造[J]. 河北地质学院学报, 1989, 01: 54~68.
Wang Zuoxun, Wu Jiyi, Lv Xichao, et al. The plate tectonics of Tianshan in China[J].Journal of Hebei College of Geology, 1989, 1: 54~68(in Chinese with English abstract).
- [6] 高俊, 钱青, 龙灵利, 等. 西天山的增生造山过程[J]. 地质通报, 2009, 12: 1804~1816.
Gao Jun, Qian Qing, Long Lingli, et al. Accretionary orogenic process of Western Tianshan, China[J]. Geological Bulletin of China, 2009, 12: 1804~1816(in Chinese with English abstract).
- [7] Gao J, Long LL, Klemd R, et al. Tectonic evolution of the South Tianshan orogen and adjacent regions, NW China: Geochemical and age constraints of granitoid rocks[J]. International Journal of Earth Sciences, 2009, 98(6): 1221~1238.
- [8] Qian Qing, Gao Jun, Xiong Xiangming, et al. Petrogenesis and tectonic settings of Carboniferous volcanic rocks north Zhaosu,

- Western Tianshan Mountains:constraints from petrology and geochemistry[J]. *Acta Petrologica Sinica*, 2006, 05: 1307–1322.
- [9] 刘静, 李永军, 王小刚, 等. 西天山阿吾拉勒一带伊什基里克组火山岩地球化学特征及构造环境[J]. *新疆地质*, 2006, 02: 105–108.
Liu Jing, Li Yongjun, Wang Xiaogang, et al. Geochemical characteristics and tectonic environment of the Yishijilike Formation volcanic rocks in the Awulale area of western Tianshan[J]. *Xinjiang Geology*, 2006, 02: 105–108(in Chinese with English abstract).
- [10] 车自成, 刘良, 刘洪福, 等. 论伊犁古裂谷[J]. *岩石学报*, 1996, 03: 478–490.
Che Zicheng, Liu Liang, Liu Hongfu, et al. Review on the Ancient Yili Rift[J]. *Acta Petrologica Sinica*, 1996, 03: 478–490 (in Chinese with English abstract).
- [11] 夏林圻, 李向民, 夏祖春, 等. 天山石炭—二叠纪大火成岩省裂谷火山作用与地幔柱[J]. *西北地质*, 2006, 01: 1–49.
Xia Linqi, Li Xiangmin, Xia Zuchun, et al. Carboniferous–Permian rift– Related volcanism and mantle plume in the Tianshan,Northwestern China[J]. *North Western Geology*, 2006, 01: 1–49(in Chinese with English abstract).
- [12] Windley B F, Allen M B, Zhang C, et al. Paleozoic accretion and Cenozoic deformation of the Chinese Tien Shan Range[J]. *Central Asia Geology*, 1990, 18(2) : 128–131.
- [13] 姜常义, 吴文奎, 张学仁, 等. 从岛弧向裂谷的变迁—来自阿吾拉勒地区火山岩的证据[J]. *岩石矿物学杂志*, 1995, 04: 289–300.
Jiang Changyi, Wu Wenkui, Zhang Xueren, et al. The change from island arc to rift valley—evidence from volcanic rocks in Awulale area[J]. *Acta Petrologica et Mineralogica*, 1995, 04: 289–300(in Chinese with English abstract).
- [14] 朱永峰, 张立飞, 郭璇, 等. 移动的古生代岛弧:新疆西南天山大哈拉军山组火山岩[C]//中国矿物岩石地球化学学会. 中国矿物岩石地球化学学会第十届学术年会论文集. 中国矿物岩石地球化学学会: 2005: 1.
Zhu Yongfeng, Zhang Lifei, Guo Xuan, et al. Mobile Xinjiang Southwest Tianshan Paleozoic island arc volcano rocks of Dahala junshan group[C]//Chinese Society of Mineralogy Petrology and Geochemistry. China mineral Rock Geochemistry Institute Tenth Annual Symposium. Chinese society of Mineralogy Petrology and Geochemistry: 2005: 1(in Chinese with English abstract).
- [15] 钱青, 高俊, 熊贤明, 等. 西天山昭苏北部石炭纪火山岩的岩石地球化学特征、成因及形成环境[J]. *岩石学报*, 2006, 05: 1307–1322.
Qian Qing, Gao Jun, Xiong Xianming, et al. Petrogenesis and tectonic settings of Carboniferous volcanic rocks from north Zhaosu, western Tianshan Mountains:constraints from petrology and geochemistry[J]. *Acta Petrologica Sinica*, 2006, 05: 1307–1322 (in Chinese with English abstract).
- [16] 孙林华, 彭头平, 王岳军. 新疆特克斯东南大哈拉军山组玄武安山岩地球化学特征:岩石成因和构造背景探讨[J]. *大地构造与成矿学*, 2007, 03: 372–379.
Sun Hualin, Peng Touping, Wang Yuejun. Geochemical characteristics of basaltic and esites from Dahala Jun Shan formation, Southea stern Tekesi(XinJiang): Petrogenesis and its tectonic significance[J]. *Geotectonica Ermatallogenesis*, 2007, 03: 372–379(in Chinese with English abstract).
- [17] 陈丹玲, 刘良, 车自成, 等. 中天山骆驼沟火山岩的地球化学特征及其构造环境[J]. *岩石学报*, 2001, 03: 378–384.
Chen Danlin, Liu Liang, Che Zicheng, et al. Geochemical characterisits and tectonic implication of Carboniferous volcanites in the Luotuogou area of Middle Tianshan[J]. *Acta Petrologica Sinica*, 2001, 03: 378–384(in Chinese with English abstract).
- [18] 张良臣, 吴乃元. 天山地质构造及演化史[J]. *新疆地质*, 1985, 03: 1–14.
Zhang Liangchen, Wu Naiyuan. The geotectonic and its evolution of TianShan[J]. *Xinjiang Geology*, 1985, 03: 1–14(in Chinese with English abstract).
- [19] 成守德, 王广瑞, 杨树德, 等. 新疆古板块构造[J]. *新疆地质*, 1986, 02: 1–26.
Cheng Shoude, Wang Guangrui, Yang Shude, et al. The paleoplate tectonic of Xinjiang[J]. *Xinjiang Geology*, 1986, 02: 1–26(in Chinese with English abstract).
- [20] 李永军, 胡克亮, 周继兵, 等. 西天山伊什基里克山早石炭世火山岩浆作用及其成矿[J]. *地球科学——中国地质大学学报*, 2010, 02: 235–244.
Li Yongjun, Hu Keliang, Zhou Jibin, et al. Early Carboniferous volcano– magmatism and related mineralization in Yishijilike mountain,Western Tianshan[J]. *Earth Science—Journal of University of Geosciences*, 2010, 02: 235–244(in Chinese with English abstract).
- [21] 新疆维吾尔自治区地质矿产开发局第二区域地质调查大队. 新疆新源县阿克塔斯—带 1:5 万区域地质矿产调查[R]. 2005. Geology and Mineral Resources Bureau of Xinjiang Uygur Autonomous Region to Develop A Second Region of Xinjiang Geological Survey Brigade. Aktas Xinyuan County Area 1:50000 Regional Reological and Mineral Survey [R]. 2005(in Chinese).
- [22] 罗刚, 李辉华, 霍加庆, 等. 新疆新源县式可布台铁矿中矿段资源/储量核实报告[R]. 2012: 12–25.
Luo Gang, Li Huihua, Huo Jiaqing, et al. The Verification Report of the Resource/reserve in Shikebutai Iron Ore of Xinyuan country, Xinjiang[R]. 2012: 12–25(in Chinese).
- [23] Ludwig K R. User's manual for Isoplot 3.00: A Geochronological Toolkit for Microsoft Excel. Berkeley Geochronology Center, Special Publication, 2003, 4: 70.
- [24] J.A.Winchester and P.A. Floyd. Geochemical discrimination of different magma series and their differentiation products using immobile elements[J]. *Chemical Geology*, 1977, (20): 325–343.
- [25] Le Bas M J, Le Maitre R W, Streckeisen A, et al. Chemical

- classification of volcanic rocks based on the total alkalisilica diagram[J]. *Journal of Petrology*, 1986, 27(3): 745–750.
- [26] Boynton W V. Geochemistry of the rare earth elements: Meteostudies[C]/Henderson P. *Rare Earth Element Geochemistry*. Amsterdam: Elsevier, 1984: 63–114.
- [27] Sun S S, McDonough W F. Chemical and isotopic systematics of oceanic basalts: Implications for mantle composition and processes[J]. *Geological Society Special Publication*, 1989, 42: 313–345.
- [28] 吴元保, 郑永飞. 锆石成因矿物学研究及其对U-Pb年龄解释的制约[J]. *科学通报*, 2004, 16: 1589–1604.
Wu Yuanbao, Zheng Yongfei. Genesis of zircon and its constraints on interpretation of U-Pb age[J]. *Chinese Science Bulletin*, 2004, 16: 1589–1604(in Chinese).
- [29] Pidgeon R T. 2480 Ma old zircons from granulite facies rocks from east Hebei Province, North China[J]. *Geological Review*, 1980, 03: 203–207.
- [30] 刘战庆, 裴先治, 李瑞保, 等. 东昆仑南缘阿尼玛卿构造带布青山地区两期蛇绿岩的LA-ICP-MS锆石U-Pb定年及其构造意义[J]. *地质学报*, 2011, 02: 185–194.
Liu Zhanqing, Pei Xianzhi, Li Ruibao, et al. LA-ICP-MS Zircon U-Pb geochronology of the two suites of ophiolites at the Buqingshan area of the A'nyemaqen orogenic belt in the southern margin of East Kunlun and its tectonic implication[J]. *Acta Geologica Sinica*, 2011, 02: 185–194(in Chinese with English abstract).
- [31] Morimoto N, Fabries J, Ferguson A K, et al. Nomenclature of pyroxenes[J]. *American Mineralogist*, 1988, 73(9/10): 1123–1133.
- [32] 蒋宗胜, 张作衡, 侯可军, 等. 西天山查岗诺尔和智博铁矿区火山岩地球化学特征、锆石U-Pb年龄及地质意义[J]. *岩石学报*, 2012, 07: 2074–2088.
Jiang Zongsheng, Zhang Zuoheng, Hou Kejun, et al. Geochemistry and zircon U-Pb age of volcanic rocks from the Chagangnuoer and Zhibo iron deposits, western Tianshan, and their geological significance[J]. *Acta Petrologica Sinica*, 2012, 07: 2074–2088(in Chinese with English abstract).
- [33] Jacks P, et al. 造山区域火山岩的主要元素及微量元素的丰度[J]. 南京大学地质科技资料, 1972.
- Jacks P, et al. Major Element Abundances Volcano Rocks in Orogenic Zone and Trace Elements[J]. Nanjing University Geological Science and Technology Information, 1972(in Chinese).
- [34] 邱家骥, 林景仟. 岩石化学[M]. 北京: 地质出版社, 1991: 1–255.
Qiu Jiaxiang, Lin Jingqian. Rock chemistry[M]. Beijing: Geological Publishing House, 1991: 1–255(in Chinese with English abstract).
- [35] Large R R, Gemmell J B, Paulick H, et al. The alteration box plot: A simple approach to understanding the relationship between alteration mineralogy and lithogeochemistry associated with volcanic-hosted massive sulfide deposits[J]. *Economic Geology*, 2001, 96(5): 957–971.
- [36] Pearce J A. Role of the sub-continental lithosphere in magma genesis at active continental margins[C]/Hawkesworth C J, Norry M J(eds.). *Continental Basalts and Mantle Xenoliths*. Shiva, Cheshire, U.K. 1983: 230–249.
- [37] 李昌年. 火成岩微量元素岩石学[M]. 武汉: 中国地质大学出版社, 1992: 1–195.
Li Changnian. Igneous Rock Trace Element Petrology[M]. Wuhan: China University of Geosciences Press, 1992: 1–195(in Chinese with English abstract).
- [38] Rottura A, Bargossi G M, Caggianelli A, et al. Origin and significance of the Permian high-K calc-alkaline magmatism in the central-eastern Southern Alps[J]. *Lithos*, 1988, 45(1/4): 329–348.
- [39] 杨学明, 杨晓勇, 陈双喜. 岩石地球化学[M]. 合肥: 中国科学技术大学出版社, 2000: 1–275.
Yang Xueming, Yang Xiaoyong, Chen Shuangxi. *Geochemistry* [M]. Hefei: University of Science and Technology China Press, 2000: 1–275(in Chinese with English abstract).
- [40] 王玉往, 王京彬, 龙灵利, 等. 新疆北部大地构造演化阶段与斑岩-浅成低温热液矿床的构造环境类型[J]. *中国地质*, 2012, 39(3): 695–716.
Wang Yuwang, Wang Jingbin, Long Lingli, et al. Tectonic evolution stages of northern Xinjiang and tectonic types of porphyry-epithermal deposits[J]. *Geology in China*, 2012, 39(3): 695–716(in Chinese with English abstract).
- [41] Han B F, Guo Z J, Zhang Z C, et al. Age, geochemistry, and tectonic implications of a late Paleozoic stitching pluton in the North Tian Shan suture zone, western China[J]. *Geological Society of America Bulletin*, 2010, 122: 627–640.
- [42] 朱志新, 董连慧, 刘淑聪, 等. 新疆西天山伊犁地块晚古生代火山岩地质特征及构造意义[J]. *新疆地质*, 2012, 03: 258–263.
Zhu Zhixin, Dong Lianhui, Liu Shucong, et al. Volcanic rock geological characteristics and tectonic significance of the late Paleozoic Yili Block in the western Tianshan, Xinjiang[J]. *Xinjiang Geology*, 2012, 03: 258–263(in Chinese with English abstract).
- [43] 赵振华, 白正华, 熊小林, 等. 西天山北部晚古生代火山-浅侵位岩浆岩⁴⁰Ar/³⁹Ar同位素定年[J]. *地球化学*, 2003, 04: 317–327.
Zhao Zhenhua, Bai Zhenghua, Xiong Xiaolin, et al. ⁴⁰Ar/³⁹Ar chronological study of Late Paleozoic volcanic-hypabyssal igneous rocks in western Tianshan, Xinjiang[J]. *Geochimica*, 2003, 04: 317–327(in Chinese with English abstract).
- [44] Zhao Zhenhua, Xiong Xiaolin, Wang Qian, et al. Underplating-related adakites in Xinjiang Tianshan, China[J]. *Lithos*, 2008, 102(1/2): 374–391.
- [45] 朱志新, 李锦轶, 董连慧, 等. 新疆西天山古生代侵入岩的地质特征及构造意义[J]. *地学前缘*, 2011, (02): 170–179.
Zhu Zhixin, Li Jinyi, Dong Lianhui, et al. Geological characteristics and tectonic significance of Paleozoic intrusive

- rocks in Western Tianshan of Xinjiang Province[J]. Earth Science Frontiers, 2011, (02): 170–179(in Chinese with English abstract).
- [46] Krner A, Windley B F, Badarch G, et al. Accretionary growth and crust formation in the Central Asian orogenic belt and comparison with the Arabian–Nubian shield[C]//Hatcher R D, Carlson M P, McBride J H, et al. 4–D Framework of Continental Crust. Geological Society of America Memoir, 2007, 200: 181–209.
- [47] 李继磊, 苏文, 张喜, 等. 西天山阿吾拉勒西段麻粒岩相片麻岩锆石 Cameca U–Pb 年龄及其地质意义[J]. 地质通报, 2009, (12): 1852–1862.
- Li Jilei, Su Wen, Zhang Xi, et al. Zircon Cameca U–Pb dating and its significance for granulite– facies gneisses from the western Awulale Mountain, West Tianshan, China[J]. Geological Bulletin of China, 2009, (12): 1852–1862(in Chinese with English abstract).
- [48] 舒良树, 朱文斌, 王博, 等. 新疆古块体的形成与演化[J]. 中国地质, 2013, 40(1): 43–60.
- Shu Liangshu, Zhu Wenbin, Wang Bo, et al. The formation and evolution of ancient blocks in Xinjiang[J]. Geology in China, 2013, 40(1): 43–60(in Chinese with English abstract).
- [49] Mullen E D. MnO/TiO₂/P₂O₅: a minor element discriminant for basaltic rocks of oceanic environments and its implications for petrogenesis[J]. Earth and Planetary Science Letters, 1983, (62): 53–62.
- [50] Wood D A. The application of a Th–Hf–Nb diagram to problems of tectomagmatic classification and to establishing the nature of crustal contamination of the British Tertiary volcanic province[J]. Earth Plant Sci. Lett., 1980, (50): 11–30.
- [51] 董连慧, 王克卓, 朱志新, 等. 新疆大型变形构造特征与成矿关系研究[J]. 中国地质, 2013, 40(5): 1552–1568.
- Dong Lianhui, Wang Kezhuo, Zhu Zhixin, et al. The relationship between the characteristics of the large– scale deformation structure and the metallogenetic processes in Xinjiang[J]. Geology in China, 2013, 40(5): 1552–1568(in Chinese with English abstract).

Geochemical characteristics and petrogenetic age of volcanic rocks in the Shikebutai iron deposit of West Tianshan Mountains

LI Xiao-linbin¹, GONG Xiao-ping¹, MA Hua-dong², HAN Qiong¹,
SONG Xiang-long¹, XIE Lei¹, FENG Jun¹, WANG Jian-she¹

(1. College of Geology and Mining Engineering, Xinjiang University, Urumqi 830049, Xinjiang, China; 2. National 305 Project Office, Urumqi 830000, Xinjiang, China)

Abstract: Located in the western part of the West Tianshan Awulale iron metallogenetic belt, the Shikebutai iron deposit is a representative deposit in this belt. It mainly occurs in the Carboniferous Yishijilike Formation volcanic rocks dominated by tuff. Based on rock geochemistry and LA–ICPMS zircon U–Pb dating of volcanic rocks in the Shikebutai iron deposit, this paper discusses the tectonic environment and petrogenetic age of the volcanic rocks. Geochemical analysis shows that most of the volcanic rocks vary from high potassium calc–alkaline volcanic rocks to shoshonite series in chemical composition. The major elements indicate that volcanic rocks are mainly composed of andesite, dacite, rhyolite and dacite, belonging to calc–alkaline series. Trace elements and rare earth elements indicate that the tectonic environment for the formation of the volcanic rocks was active epicontinent volcanic arc. LA–ICPMS zircon U–Pb dating shows that ²⁰⁶Pb/²³⁸U weighted average ages of volcanic rocks are 301±1Ma and 313±2Ma, suggesting that volcanic rocks in this deposit were formed in early Late Carboniferous. Combined with regional geological data, the authors hold that the high–K calc–alkaline volcanic rocks of shoshonite series in the ore district may be the product of the late subduction of continental arc magmatism, and the tectonic environment for the formation of the volcanic rocks was active epicontinent arc. The chemical characteristics of the volcanic rocks are on the whole similar to features of Lower Carboniferous Dahalajunshan Formation volcanic rocks.

Key words: LA–ICPMS; geochemistry; Yishijilike Formation; Shikebutai iron deposit; West Tianshan Mountains

About the first author: LI Xiao-linbin, male, born in 1989, master, mainly engages in the study of earth exploration and information technology; E-mail: lb5310@sina.com.

About the corresponding author: GONG Xiao-ping, male, born in 1963, doctor, professor, engages in metallogenetic prediction based on comprehensive information; E-mail: gxiapinol@63.com.